Quantifying the degree of nanofiller dispersion by advanced thermal analysis: application to polyester nanocomposites prepared by various elaboration methods†

Hans E. Miltner,[a] Nick Watzeels,[a] Anne-Lise Goffin,[b] Emmanuel Duquesne,[b] Samira Benali,[b] Philippe Dubois,[b] Hubert Rahier[a] and Bruno Van Mele*[a]

Received 31st May 2010, Accepted 16th August 2010
DOI: 10.1039/c0jm01673j

An innovative thermal analysis methodology is applied for the characterization of poly(ε-caprolactone) (PCL) nanocomposites containing layered silicates, needle-like sepiolite or polyhedral oligomeric silsesquioxane (POSS) nano-cages, aiming at assessing the key factors affecting nanofiller dispersion and nanocomposite properties. This methodology takes benefit of the fact that—for a given nanofiller aspect ratio—the magnitude of the excess heat capacity recorded during quasi-isothermal crystallization is directly related to the occurrence of pronounced changes to the PCL crystalline morphology. The extent of these changes, in turn, directly depends on the amount of matrix/filler interface and can therefore be considered a reliable measure for the degree of nanofiller dispersion, as supported by complementary morphological characterization. The importance of processing parameters is demonstrated in a comparative study using various melt processing conditions, evidencing the need for high shear to effectively exfoliate and disperse individual nanoparticles throughout the polymer matrix. Furthermore, the choice of the nanocomposite elaboration method is shown to profoundly affect the final morphology, as illustrated in a comparison between nanocomposites prepared by melt mixing, by *in situ* polymerization and by a masterbatch approach. Grafting PCL onto the filler strongly enhances its dispersion quality as compared to conventional melt mixing; subsequently further dispersing such grafted nanohybrids into the polymer matrix through a masterbatch approach provides a highly efficient method for the elaboration of well-dispersed nanocomposites. Finally, the crucial issue of interfacial compatibility is addressed in a comparison between various surface-treated layered silicates, showing that high degrees of filler dispersion in a PCL matrix can only be achieved upon polar modification of the silicate.

Introduction

With a structure almost free of defects, nano-sized objects individually display exceptional properties. At the same time, the highest property improvements in current materials are potentially achieved by their modification at almost molecular level. The incorporation of nano-sized structures into traditional polymeric materials may therefore provide a seemingly straightforward and highly efficient method to simultaneously improve a wide span of material properties. In view of the tremendous wealth of natural as well as man-made nanostructures, the possibilities for conceiving novel nanocomposite materials are almost unlimited, potentially paving the way towards unprecedented performance levels and functional materials with well-adjusted properties for specific applications. The challenge, however, consists of retaining the ideal properties of the nanoscale building blocks in the macroscale composites.

Since their introduction some 20 years ago, polymeric nanocomposites containing organically modified layered silicates[1] and carbon nanotubes[2] have attracted tremendous research effort in both academia and industry. More recently, other types of nanostructures have also been gaining increasing attention, for instance needle-like sepiolite clay[3] or polyhedral oligomeric silsesquioxane (POSS) nano-cages.[4] By their incorporation, a wide range of property enhancements has been reported over the years, with nanocomposites potentially outranging the unfilled matrix polymer on several fronts. Depending on the considered matrix and nanofiller types, nanocomposites may display superior mechanical properties, improved barrier properties, raised heat distortion temperature, increased crystallization rate, effective flame retardant behavior, outstanding electrical conductivity, increased glass transition temperature, *etc.*[5–8] The origin of such superior properties, at filler loadings much smaller than in conventional micro-composites, is related to the small size and high aspect ratio of the nanoparticles. Indeed, the enormous specific surface area they provide potentially ensures a high degree of polymer–filler interaction and may result in

[a]*Vrije Universiteit Brussel (VUB), Department of Materials and Chemistry (MACH)—Physical Chemistry and Polymer Science (FYSC), Pleinlaan 2, B-1050 Brussels, Belgium. E-mail: bvmele@vub.ac.be; Fax: +32-(2)-629.32.78; Tel: +32-(2)-629.32.76*
[b]*University of Mons (UMONS), Laboratory of Polymeric and Composite Materials (LPCM)—Center of Innovation and Research in Materials and Polymers (CIRMAP), Place du Parc 20, B-7000 Mons, Belgium*
† This paper is part of a *Journal of Materials Chemistry* themed issue on Advanced Hybrid Materials, inspired by the symposium on Advanced Hybrid Materials: Stakes and Concepts, E-MRS 2010 meeting in Strasbourg. Guest editors: Pierre Rabu and Andreas Taubert.

a tremendous amount of interphase material with altered physical and chemical properties.

Getting the nanoparticles well-dispersed in order to exploit the high specific surface of the filler is therefore a prerequisite for achieving significant property enhancement. This is, however, also one of the challenging difficulties when preparing thermoplastic nanocomposites. Several strategies can be envisaged to maximize the achievable degree of filler dispersion.

A first key factor turned out to be the interfacial compatibility between polymer matrix and reinforcement, which requires careful adjustment by, *e.g.*, modifying the surface characteristics of the filler particles.[9–12]

The choice of the method by which the constituents are combined into a homogeneous and macroscopically uniform material is a second key aspect, which to a large extent determines the outcome for any polymer–filler combination. A large variety of approaches has been envisaged: direct mixing of the individual components,[13] *in situ* nanoparticle generation within a polymer matrix,[14] grafting of macromolecules onto nano-sized filler particles,[15,16] *in situ* synthesis of the polymer in the presence of nanoparticles,[17,18] various masterbatch approaches,[19–22] *etc.*

For a given preparation method, finally, the choice of processing conditions is a third key parameter governing the achievable degree of filler dispersion throughout a polymer matrix. For instance, properly adjusted processing conditions dramatically improve the efficiency of extrusion-based melt mixing,[23,24] whereas sonication was demonstrated to be essential in many solution or latex-based mixing methods.[25]

We previously reported on the mechanical, thermal and rheological properties of nanoparticle-reinforced poly(ε-caprolactone), a biodegradable and biocompatible aliphatic polyester.[26–30] In view of its widespread applicability, the melt mixing method was generally preferred for the preparation of nanocomposites containing layered silicates, sepiolite, carbon nanotubes and POSS nano-cages. The particles were observed to induce significant changes to the crystalline morphology of the matrix polymer, to an extent related to their aspect ratio, to their dispersion quality, and to the amount of polymer–filler contact surface provided. More specifically, the crystalline/amorphous interface was found to strongly increase in the presence of *well-dispersed* high aspect ratio nanoparticles.[27]

The present article aims at demonstrating how a newly developed thermal analysis methodology can be applied for quantifying the degree of nanofiller dispersion throughout the polymeric matrix. For this purpose, nanocomposites prepared by melt mixing, *in situ* polymerization and masterbatch approaches will be investigated and their thermal characteristics compared in relation to the achieved filler dispersion quality. In addition, the importance of filler modification, affecting its compatibility with the matrix material, will be highlighted for a large number of organically modified layered silicates prepared under optimized processing conditions.

Experimental part

Materials

For nanocomposites prepared by melt mixing, poly(ε-caprolactone) commercialized under the trade name CAPA®6500 was obtained from Solvay Caprolactones (presently Perstorp Caprolactones/UK, M_n = 47.500 and M_w = 84.500 g mol^{-1} according to the manufacturer).

Various layered silicates were obtained from Southern Clay Products (presently Rockwood Additives Inc.)/USA: Cloisite®Na^+, a natural montmorillonite with a cation exchange capacity (CEC) of 92 meq per 100 g; Cloisite®10A, exchanged by benzyl dimethyl tallowalkyl ammonium; Cloisite®25A, exchanged by dimethyl 2-ethylhexyl hydrogenated tallowalkyl ammonium; and Cloisite®30B, exchanged by methyl bis(2-hydroxyethyl) tallowalkyl ammonium. In addition, Cloisite®Na^+ was exchanged by dimethyl 2-hydroxyethyl octadecyl ammonium to yield a modified clay termed Cloisite®OCT. This ion exchange reaction was conducted in aqueous medium according to a procedure described elsewhere.[21]

Bentone®108, a natural hectorite exchanged with dimethyl bis(hydrogenated tallowalkyl) ammonium, was obtained from Elementis Specialties/USA.

Laponite®RD, a synthetic sodium hectorite from Southern Clay Products (presently Rockwood Additives Inc./USA), and Somasif®ME100, a synthetic sodium fluoromica from Co-op Chemical Ltd. (Japan), were organically modified by dimethyl 2-hydroxyethyl octadecyl ammonium to yield Laponite®OCT and Somasif®OCT. For all layered silicates the organic contents were determined by thermogravimetric analysis (TGA).

Needle-like sepiolite clay was obtained from Tolsa/Spain and was used as-received or after amino-functionalization according to a reported procedure (see also hereafter: Nanohybrid synthesis).[29,31]

Aminopropyl heptakis(isobutyl) POSS, termed POSS–NH_2 (97% purity), was obtained from Hybrid Plastics (USA) and was used without further treatment.

Nanohybrid synthesis

The procedures for the *in situ* synthesis of the nanohybrids have been previously reported in detail.[22,29,32–34]

In the case of layered silicate nanocomposites,[32,34] ε-caprolactone was polymerized in bulk in the presence of various amounts of Cloisite®30B (1–10 wt% inorganic content, 24 h at room temperature). The polymerization was activated by dibutyltin dimethoxide in toluene solution, with the hydroxyl functions of the organic modifier acting as co-initiator/chain transfer agents. As a result, the number-average molar mass M_n of the obtained grafted PCL decreases with increasing clay content.[32] A grafted Cloisite®30B–PCL masterbatch with an inorganic content of 25 wt% was prepared following an adapted synthesis procedure (M_n of the grafted PCL chains ~1500 g mol^{-1}).[22]

For sepiolite nanocomposites,[29] the filler was first amino-functionalized using γ-aminopropyltriethoxysilane. After purification the aminopropyl-modified sepiolite was reacted with ε-caprolactone in the presence of tin(II) bis(2-ethylhexanoate) in toluene solution at 100 °C. Soxhlet extraction was subsequently used to remove the non-grafted PCL chains. The inorganic content in the obtained grafted sepiolite–PCL masterbatch was determined by TGA to be 40 wt%.

Finally, in the case of POSS nanocomposites,[33] ε-caprolactone was polymerized in toluene solution at 100 °C in the presence of POSS–NH_2 and catalyzed by tin(II) ethylhexanoate. The POSS

end-capped PCL was recovered from heptane precipitation. Two types of POSS–PCL masterbatches were prepared according to the described procedure, with polymerization degrees of DP = 40 and 80 and with inorganic contents of 19.2 and 9.6 wt%, respectively.

Nanocomposite preparation

The nanocomposites investigated throughout this work were either directly prepared by *in situ* polymerization (as described above), or alternatively by melt mixing techniques. In addition, a masterbatch approach was followed, in which nanohybrids prepared by *in situ* polymerization were subsequently incorporated into a commercial PCL matrix by melt mixing. Throughout the article, compositions are expressed in terms of the inorganic filler content in the respective samples; a hyphen between the constituents is exclusively used for PCL-grafted systems, *i.e.*, *in situ* polymerized nanocomposites and masterbatches (the latter are further identified by the abbreviation MB).

The experimental procedure for the melt mixing and masterbatch approaches is briefly summarized (note that all samples were extensively dried under vacuum prior to processing).

PCL/layered silicate composites were prepared by mechanical kneading using an AGILA two-roll mill at 130 °C for 10 min.[26] In a second series of samples, melt mixing conditions have been adjusted to fine-tune the filler dispersion quality. Those samples were prepared at 130 °C using a lab-scale twin-screw DSM Xplore Micro-Compounder (15 cm^3, N_2 purge, variable residence time and screw rotation speed).

PCL/sepiolite nanocomposites were prepared by melt blending using a MiniLab Rheomex CTW5 twin screw extruder from Thermo-Haake (80 °C, 10 min) and subsequently compression-molded using an AGILA PE 20 hydraulic press. A similar extrusion procedure was used for the preparation of PCL/POSS nanocomposites (90 °C, 10 min, followed by compression molding).

Characterization techniques

Morphological characterization was performed by Transmission Electron Microscopy (TEM, Philips CM200, accelerator voltage 120 kV) as well as by tapping-mode Atomic Force Microscopy (AFM, Veeco Dimension 3100). Samples for TEM and AFM imaging were prepared at −100 °C using a LEICA Ultracut UCT ultra-cryomicrotome.

Wide-Angle X-ray Diffraction (WAXD) was performed using a Siemens D5000 diffractometer with Cu K_α-radiation, operating at 40 kV and 40 mA.

Thermal characterization using Modulated Temperature Differential Scanning Calorimetry (MTDSC) was performed using a TA Instruments Q2000 DSC. For quasi-isothermal experiments the instrument was equipped with a Refrigerated Cooling System (RCS), whereas a Liquid Nitrogen Cooling System (LNCS) was used for non-isothermal experiments. The instrument was purged with Nitrogen or Helium gas (25 ml min^{-1}), respectively. Temperature and enthalpy calibration were performed using an Indium standard. Sapphire disks were used for heat capacity calibration. The selected temperature modulation conditions were an amplitude of ±0.5 °C and a period of 60 s. Prior to measurement, all samples were dried under vacuum at 65 °C for one night. The experiments were initiated by a one hour stay in the melt at 130 °C to fully erase the thermal history of the samples; thermal degradation of the PCL during this pre-treatment of the samples can be excluded based upon GPC data.

Dynamic mechanical analysis (DMA) on compression molded samples was conducted in single cantilever mode on a TA Instruments Q800 DMA. The instrument was calibrated for compliance according to a manufacturer-defined procedure; temperature calibration was performed by means of the melting transition of a Gallium standard. The bending modulus of the nanocomposite samples was determined isothermally at 20 °C at a frequency of 1 Hz.

Results and discussion

It is well-established that filler dispersion quality—in addition to filler type—is a most crucial parameter in determining whether or not significant property enhancements can be reached with regard to the unfilled matrix. We previously reported on the effect of filler aspect ratio on the interphase formation and thermal properties in PCL nanocomposites prepared by melt mixing.[27] It is the aim of the present work to shed light on the equally important aspect of filler dispersion state, which—in addition to being determined by interfacial compatibility issues—is to a large extent governed by the selected nanocomposite preparation method. A wide range of PCL-based materials is investigated for this purpose: (i) nanocomposites prepared by melt mixing provide insight into the effect of processing conditions; (ii) nanocomposites prepared by *in situ* polymerization and masterbatch mixing evidence the role of the preparation method; and (iii) nanocomposites based on layered silicates with different surface modifications demonstrate the importance of interfacial compatibility. In all three cases the focus will be on the determination of the achieved filler dispersion state and on the resulting thermal characteristics of the nanocomposites. An innovative thermal analysis method will be used for this purpose, backed by complementary evidence from 'classical' morphological techniques.

Methodology for the evaluation of filler dispersion

We previously reported on a novel thermal analysis methodology for the characterization of polymeric nanocomposites, which is based on quasi-isothermal crystallization experiments by means of MTDSC.[27,30,35–37] Instead of attaining the anticipated baseline level reflecting the developed degree of crystallinity, it was observed that—during quasi-isothermal crystallization of certain polymeric systems—the recorded heat capacity signal remains at a level much higher than expected due to the presence of an *excess* contribution superimposed onto the *baseline* heat capacity. The measured heat capacity is therefore termed apparent heat capacity, *i.e.*, $C_p^{apparent} = C_p^{baseline} + C_p^{excess}$, which depends on time and temperature and changes with the progress of the transformation.

The origin of C_p^{excess} is related to the occurrence of latent heat effects associated with melting and crystallization on the time-scale of the imposed MTDSC temperature modulation,[38–40] therefore contributing to the heat capacity signal (a complete

description of the extracted MTDSC signals can be found in literature[41,42]).

Applied to the characterization of polymeric nanocomposites, our methodology consists of quantitatively evaluating the equilibrium value of C_p^{excess} at the end of the quasi-isothermal crystallization experiment, *i.e.*, long after completion of the irreversible crystallization when the heat flow signal has attained its baseline level. In this final stage of crystallization, the determined C_p^{excess} value is exclusively due to a fast process of reversible melting/crystallization of a small polymer fraction on the timescale of the imposed temperature modulation.[43]

The considered heat capacity levels are illustrated in Fig. 1 for unfilled PCL and for a melt-mixed PCL nanocomposite containing 5 wt% of Cloisite®30B. As indicated, C_p^{excess} is evaluated with respect to the calculated $C_p^{baseline}$ after 1000 min of quasi-isothermal crystallization,[44] taking the developed degree of crystallization into account as determined from a subsequent heating experiment.

For poly(amide)-6 and poly(ethylene-*co*-vinyl acetate) matrices, a decrease in C_p^{excess} was noticed upon incorporation of nano-sized filler particles.[35–37] This *decrease* was attributed to a reduction in the polymer chain segment mobility as a result of polymer/filler interaction. In the particular case of PCL nanocomposites, however, we previously demonstrated that the presence of nano-sized filler particles leads to a marked *increase* in C_p^{excess}, as can be appreciated from Fig. 1 for an organically modified layered silicate.[27] This increase was shown to be due to a modification of the crystalline morphology of the PCL matrix in the presence of filler particles, the extent of which depends upon the filler type, *i.e.*, its aspect ratio. It was indeed demonstrated that the presence of filler particles imposes considerable constraints to the crystallization of the PCL matrix in the *interphase* region, promoting the growth of subsidiary crystalline lamellae of reduced stability. Moreover, these morphological changes were demonstrated to result in an increase in the amount of crystalline/amorphous interface which, along with the lesser perfection of the crystalline lamellae, allows a larger fraction of the matrix polymer to take part in the reversible melting/crystallization phenomenon on the timescale of the imposed temperature modulation. In effect, the sheer presence of filler particles could as such be held responsible for the increased C_p^{excess} in the considered PCL nanocomposites, as well as for the formation of an important *rigid amorphous fraction*, *i.e.*, a part of the amorphous fraction of the matrix polymer that is no longer capable of devitrifying at the bulk glass transition temperature of PCL due to a significantly reduced chain segment mobility.[27]

Since, for a given type of nanofiller, the imposed constraints to the crystallization also depend upon the amount of polymer/filler interface, the developed methodology will allow us to draw conclusions with respect to the degree of filler dispersion for the various nanocomposites investigated in the present work. The method is therefore extremely valuable for investigating the importance of processing and nanocomposite preparation conditions, as well as for demonstrating the importance of matrix/filler compatibility.

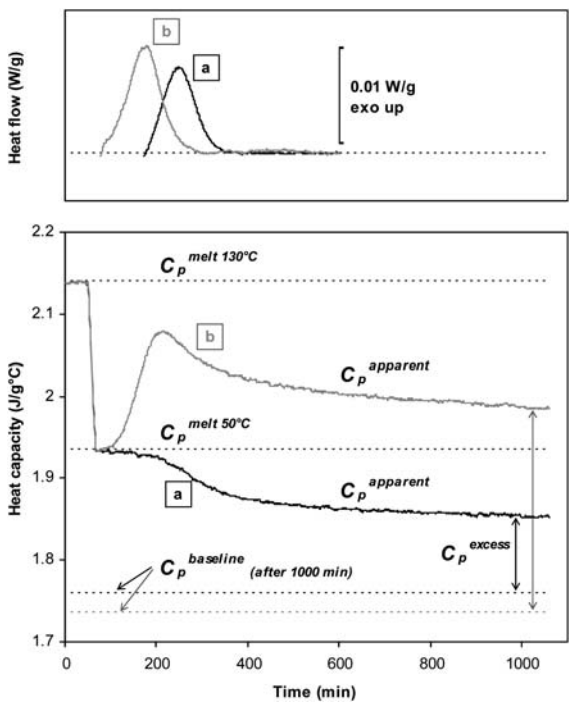

Fig. 1 MTDSC heat flow (*top*) and heat capacity (*bottom*) signals during quasi-isothermal crystallization of PCL (trace *a*, *black*) and of a nanocomposite containing 5 wt% of Cloisite®30B clay (trace *b*, *grey*). The experiment was conducted at 50 °C with an imposed temperature modulation of ±0.5 °C per 60 s. The figure shows the considered heat capacity levels with the employed nomenclature (see explanations in text): $C_p^{apparent}$ is the recorded signal; $C_p^{baseline}$ was determined at the end of the quasi-isothermal experiment to account for the developed degree of crystallinity (calculated lines drawn in the color of the corresponding samples).

Nanocomposites by melt mixing: effect of processing conditions

Nanocomposites of PCL containing layered silicates have been prepared by melt mixing using a lab-scale twin screw extruder equipped with co-rotating conical screws. A fixed composition of 5 wt% of Cloisite®30B was selected in order to allow a proper comparison between samples prepared under variable processing conditions.

Residence time. A first series of nanocomposites was prepared under high shear rate conditions at a maximum screw rotation speed of 245 rpm. A recirculation channel allows the extruder to be operated in batch mode for a user-defined residence time, after which the sample is unloaded *via* the die. The lower part of Fig. 2 shows the WAXD profiles for a series of samples run under identical conditions for different residence times. At low residence times a clear diffraction peak can be observed in the 2–3° 2θ region, attesting for the presence of intercalated clay tactoids. Upon increasing the residence time in the extruder, the WAXD peak position gradually shifts to lower angle, evidencing a progressive increase in the gallery spacing. Eventually the marked peak vanishes, suggesting that a highly disordered and most likely exfoliated dispersion state is achieved after a residence time of one hour, as has been confirmed by TEM imaging.[30] Note that GPC measurements did not reveal significant thermal degradation of PCL as a result of increasing residence times (data not shown herewith).

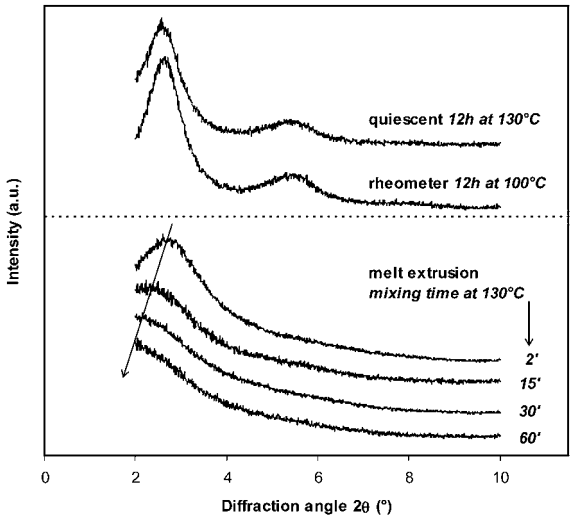

Fig. 2 WAXD patterns for a series of PCL nanocomposites containing 5 wt% of Cloisite®30B prepared by melt mixing, either quiescent or under rheometer shear flow (top), and by melt extrusion for varying residence times (bottom). The traces are shifted with respect to one another for clarity; the arrow indicates the shifting diffraction peak position.

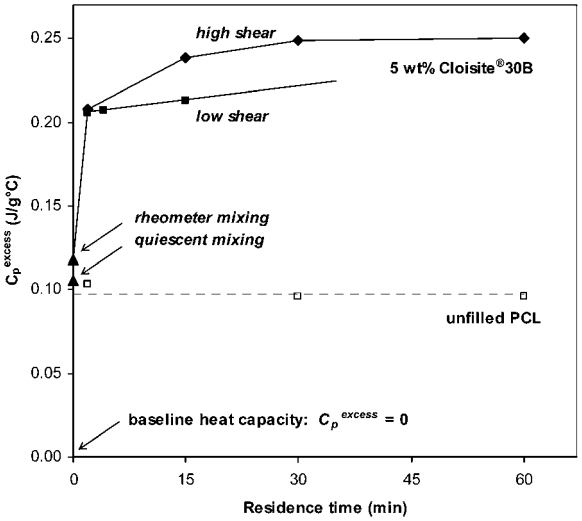

Fig. 3 C_p^{excess} from quasi-isothermal crystallization experiments (1000 min at 50 °C under a temperature modulation of ±0.5 °C per 60 s) for unfilled PCL (open symbols, melt extruded samples) and nanocomposites containing 5 wt% of Cloisite®30B (full symbols). The filled samples were prepared by either quiescent or rheometer-sheared mixing (▲, indicated by arrows and plotted on the ordinate for clarity), or by melt extrusion under low shear (■) or high shear (◆) conditions for varying residence times.

For the sake of comparison, the upper part in Fig. 2 shows two samples of same composition prepared on a parallel plate rheometer (5 wt% of Cloisite®30B powder 'sandwiched' between two PCL films), either by quiescent mixing (12 h at 130 °C) or under shear (12 h at 100 °C, imposed shear rate of 1 s^{-1}). Both samples show clear diffraction peaks attesting for an intercalated morphology. Moreover, the achieved inter-gallery spacing is very comparable, irrespective of whether the sample was prepared under rheometer shear flow (d_{001} = 3.32 nm) or under quiescent mixing conditions (d_{001} = 3.36 nm).

This series of samples was further evaluated by means of the novel MTDSC-based methodology. Fig. 3 shows the excess heat capacity C_p^{excess}, determined at equilibrium after 1000 min of quasi-isothermal crystallization. An excess heat capacity can be observed for all samples (with C_p^{excess} clearly located above the baseline value $C_p^{excess} = 0$, as indicated). The magnitude of C_p^{excess} moreover increases in the filled samples, even though it is very moderate for the quiescently mixed sample and only slightly higher for the rheometer-sheared sample. For nanocomposite samples prepared by melt extrusion, however, an important increase in C_p^{excess} up to a plateau level is noticed upon increasing the residence time, whereas this does not affect C_p^{excess} of the unfilled PCL (note that the data for the latter series also convincingly illustrate the high reproducibility of the MTDSC measurements).

We reported on the origin of C_p^{excess} in PCL nanocomposites in a previous paper, showing that it is related to an alteration of the crystalline morphology as a result of constraints imposed by the filler particles. The associated changes to the *amount* and *nature* of the crystalline/amorphous interface were shown to increase the amount of material that participates in the process of reversible melting/crystallization.[27] Accordingly, a higher increase in C_p^{excess}—for a sample composition remaining unchanged (as in Fig. 3) — reflects a proportionally stronger modification of the crystalline morphology of the PCL matrix; it can as such be directly related to an increased degree of filler dispersion. In this respect, the modest increase in C_p^{excess} for the samples prepared under quiescent or rheometer-sheared mixing conditions points at a very limited dispersion state, confirming the above WAXD data. On the other hand, a much higher dispersion quality is achieved in the melt-extruded samples; the plateau value in C_p^{excess} attained after residence times between 30 min and one hour suggests that further increasing the residence time is not beneficial in further improving the dispersion quality. This result is in full agreement with the complete disappearance of the WAXD diffraction peak in Fig. 2.

Shear stress. The importance of shear could already be partly appreciated from Fig. 3. A quiescently mixed PCL/silicate sample did hardly show any increase in C_p^{excess} in comparison with the unfilled matrix (data point represented on the ordinate axis in Fig. 3). On the other hand, a comparable sample prepared in the rheometer under a modest shear flow did show a slight increase in C_p^{excess}, evidencing a slight improvement in the dispersion quality. The true effect of shear can, however, best be appreciated by comparing samples prepared by melt extrusion: for samples of equal composition and for constant residence time, an increase in C_p^{excess} is noted to an extent depending on the shear stress during melt processing. The latter can be evaluated from an axial force recorded during mixing.[45] The data points denoted with *low shear* in Fig. 3 were run at a screw rotation speed of 50 rpm, moreover in an extruder which was not fully loaded. The recorded axial force for those experiments was *ca.* 4000 N. The *high shear* samples, on the other hand, were processed in the same extruder loaded at maximum capacity and at a screw rotation speed of 245 rpm. The recorded axial force amounted to almost 7000 N. Clearly, for a given residence time within the extruder, a higher shear stress results in an improved filler dispersion state, as evidenced by the higher C_p^{excess} recorded (Fig. 3).

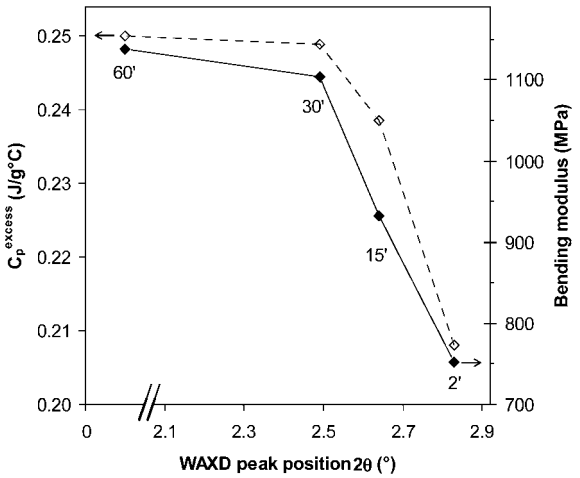

Fig. 4 C_p^{excess} (◇) and bending modulus (◆) as a function of WAXD peak position for melt-mixed PCL nanocomposites containing 5 wt% of Cloisite®30B. The residence time in the extruder is indicated for each data point. No WAXD peak was observed after 60 min residence time; the data point was therefore plotted at a 2θ angle below 2° for clarity.

Properties. The importance of filler dispersion quality in relation to property enhancement can be appreciated by evaluating the bending modulus of the prepared samples. Fig. 4 shows the bending modulus determined by DMA for samples extruded under high shear and for varying residence times (as indicated in the figure for each data point). Clearly, increasing the residence time leads to a higher improvement in mechanical properties. This is undoubtedly a result of the improved filler dispersion quality, as it is well-correlated with the position of the WAXD diffraction peak. Note that C_p^{excess} follows a very similar trend, confirming that it is indeed a reliable measure for the degree of filler dispersion and therefore correlated with the final properties of the nanocomposite.

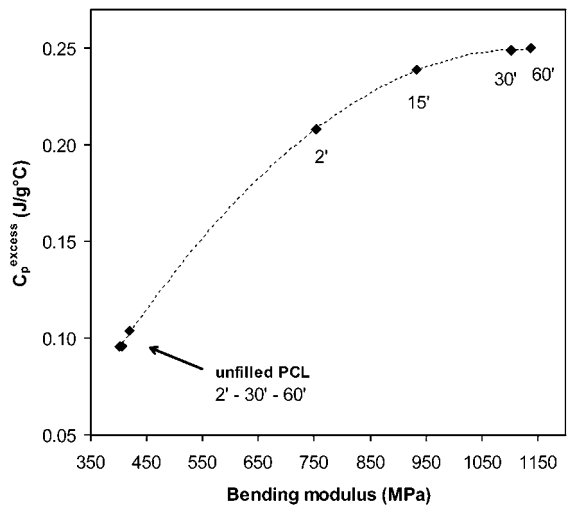

Fig. 5 C_p^{excess} from quasi-isothermal crystallization plotted against the bending modulus from dynamic mechanical analysis for unfilled PCL and nanocomposites containing 5 wt% of Cloisite®30B. The residence time in the extruder is indicated for each data point.

Fig. 5 illustrates the observed correlation between C_p^{excess} and bending modulus for samples prepared by melt extrusion under high shear conditions for various residence times (including unfilled PCL samples). Interestingly, for the same series of samples—and despite its demonstrated value for characterizing nanofiller dispersion—dynamic rheometry was not able to evidence any difference between their rheological behaviors in relation to extruder residence time (data not shown), suggesting that it is less well suited for investigating subtle changes in the degree of filler dispersion, especially at higher filler loadings.[30]

Melt mixing *vs. in situ* polymerization: effect of matrix preparation

An alternative method for preparing PCL nanocomposites consists of directly synthesizing the PCL matrix *in situ* in the presence of the nano-sized filler. The preparation of such nanohybrids was reported elsewhere.[32] It was demonstrated that the hydroxyl groups of the organic modifier in Cloisite®30B co-initiate the ring opening polymerization of ε-caprolactone. As a result, the molar mass of the matrix decreases with increasing filler content. To overcome this issue, *in situ* synthesized nanohybrids can also be incorporated into commercial PCL by melt mixing techniques in a so-called masterbatch approach, thus avoiding any alteration to the intrinsic properties of the matrix.

Layered silicates. PCL nanocomposites prepared by melt mixing were directly compared with equivalent samples prepared by *in situ* polymerization and by a masterbatch approach. Fig. 6 shows the C_p^{excess} levels recorded for samples containing various loadings of Cloisite®30B. The magnitude of C_p^{excess} increases with increasing filler content, reflecting an increase in polymer/filler contact surface, which in turn affects the crystalline morphology and the crystalline/amorphous interface.[27] In this

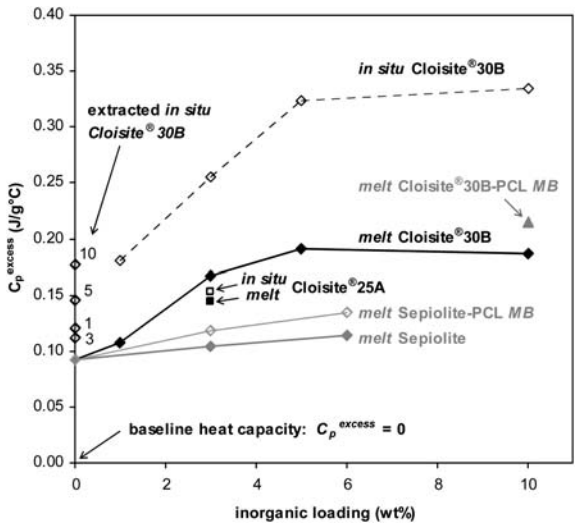

Fig. 6 C_p^{excess} determined from quasi-isothermal crystallization experiments for various PCL nanocomposites prepared by melt mixing (*melt*), by *in situ* polymerization (*in situ*) and by the masterbatch approach (*melt MB*, denoted with a hyphen between the constituents). The MTDSC experiments were conducted at 50 °C with a temperature modulation of ±0.5 °C per 60 s.

respect, the leveling off at higher loading indicates an incomplete filler dispersion, limiting the amount of polymer/filler contact surface (*e.g.*, in an intercalated rather than exfoliated nanocomposite morphology).[30]

When considering the different preparation methods, it also clearly appears from Fig. 6 that samples prepared by *in situ* polymerization show considerably higher C_p^{excess} levels than their counterparts prepared by melt mixing. This indicates that much higher degrees of filler dispersion are achieved by the former method, as illustrated by the tapping-mode AFM image in Fig. 7a and in full agreement with earlier observations by WAXD and TEM (*exfoliated* by *in situ*, *vs. intercalated/exfoliated* by melt mixing).[26,32] Note that the higher C_p^{excess} in the *in situ* samples is almost exclusively related to the presence of well-dispersed layered silicates, rather than to originate from molar mass differences between the PCL matrices in all samples.

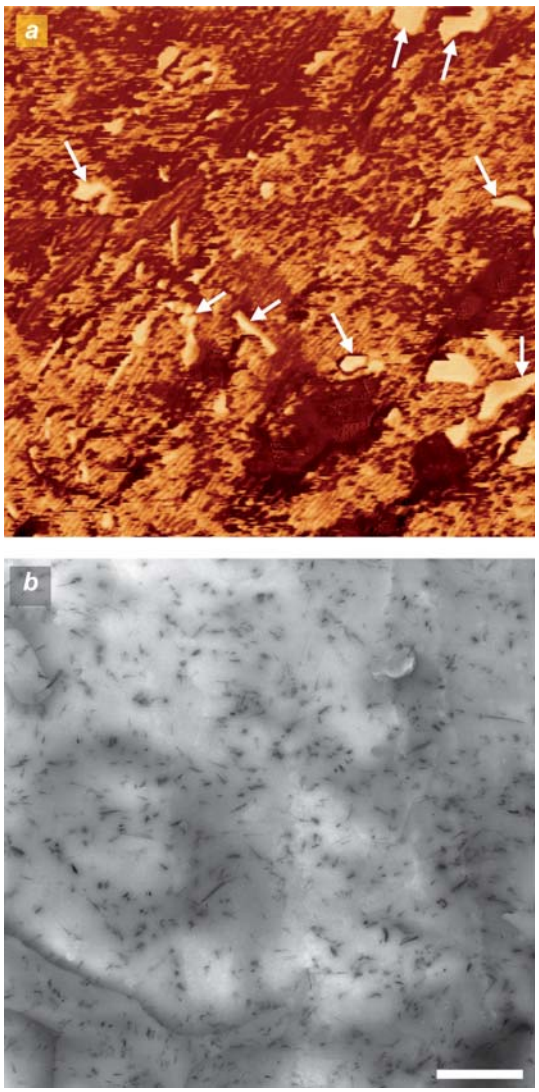

Fig. 7 (a) Tapping-mode AFM image showing the surface morphology of a PCL nanocomposite containing 3 wt% of Cloisite®30B as obtained from *in situ* polymerization (*in situ* Cloisite®30B); surface area: 1 × 1 μm²; the arrows show a number of individual silicate platelets. (b) TEM micrograph of a PCL sample filled with 3 wt% of a sepiolite–PCL masterbatch; scale bar: 1000 nm.

Indeed, as indicated in Fig. 6, the *in situ* polymerized PCL was recovered by a reversed ion exchange reaction,[32] after which C_p^{excess} is clearly found to be much lower than in the corresponding nanocomposites. The data in Fig. 6 do suggest a certain molar mass dependency, however, indicating that the process causing C_p^{excess} is to some extent also related to the kinetics of PCL crystallization.

Fig. 6 also shows the C_p^{excess} level attained after incorporation of 10 wt% of Cloisite®30B by the masterbatch approach.[20] In this case, the masterbatch itself was first synthesized by *in situ* polymerization (25 wt% loading) and subsequently diluted in commercial PCL by melt mixing to reach the final composition. As can be noticed in Fig. 6, the degree of filler dispersion is appreciably better than in the sample prepared by melt mixing alone. Note that the C_p^{excess} level attained for the masterbatch itself at 25 wt% loading (0.196 J g^{-1} °C^{-1}) is slightly lower than after dilution to a loading of 10 wt% (0.215 J g^{-1} °C^{-1}), evidencing the physical impossibility of achieving a proper dispersion quality at such high loading.

Fig. 6 also plots the C_p^{excess} level reached upon incorporation of 3 wt% of Cloisite®25A clay. A value slightly below that of Cloisite®30B is observed, indicating a lower degree of filler dispersion due to the lower compatibility of this non-polar silicate with the polar PCL matrix (see discussion in a subsequent paragraph). Even the *in situ* polymerization approach does not significantly improve the dispersion quality. The reason is that, due to the absence of hydroxyl moieties in this organically modified clay, PCL chains are no longer grafted onto the silicate surface.[32] Therefore, unlike in Cloisite®30B, the growing PCL chains do not have the ability to swell and eventually exfoliate the clay tactoids in the course of the *in situ* polymerization.

Needle-like sepiolite clay and POSS. In a previous article we extensively reported on the effect of filler aspect ratio on C_p^{excess}.[27] It was demonstrated that needle-like sepiolite and POSS nanocages have a much more limited effect on the quasi-isothermal crystallization of PCL than, for instance, layered silicates or multi-walled carbon nanotubes. The reason is probably the fact that the lower aspect ratio of these particles has a much more limited effect on the crystalline morphology of the PCL matrix, imposing fewer constraints onto its crystallization. The associated effect on the crystalline/amorphous interface is therefore assumed to be less.[27]

The results for sepiolite clay are plotted in Fig. 6; the C_p^{excess} levels can be directly compared with those attained with Cloisite®30B. Only a very limited increase in C_p^{excess} is noticed for samples prepared by direct melt mixing, despite an apparently well-dispersed morphology.[29] The C_p^{excess} effect is slightly more pronounced for samples prepared by the masterbatch approach, in which the PCL-grafted sepiolite (40 wt% loading) is diluted into commercial PCL by melt mixing. Based on TEM observation (*e.g.*, Fig. 7b), however, the dispersion state is visually equivalent to that in the melt mixed samples,[29] suggesting the high sensitivity of the presented C_p^{excess} methodology to evidence subtle changes in the degree of filler dispersion. This sensitivity is a direct result of the connection between filler dispersion and constrained crystallization, which is in turn further amplified by the profound effect it has on the crystalline/amorphous interface, hence, on C_p^{excess}.

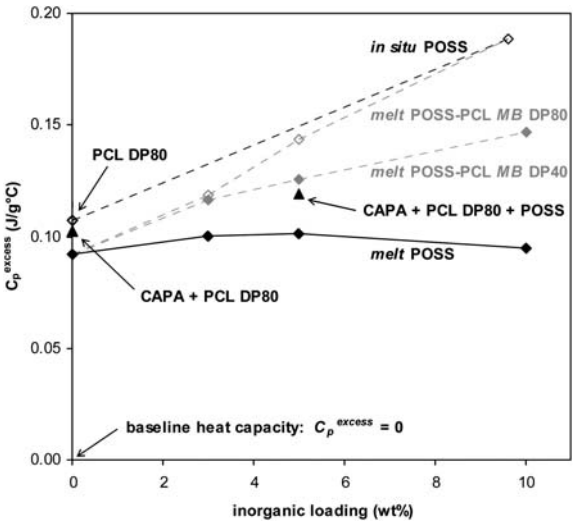

Fig. 8 C_p^{excess} from quasi-isothermal crystallization (50 °C ± 0.5 °C per 60 s) for various PCL/POSS nanocomposites prepared by melt mixing (*melt*), by *in situ* polymerization (*in situ*) and by the masterbatch approach (*melt MB*, denoted with a hyphen between the constituents). In addition, the figure shows data for a PCL homopolymer of DP = 80, as well as for binary and ternary mixtures with commercial PCL (denoted CAPA) and POSS–NH_2 (see explanations in text).

Fig. 8 shows the C_p^{excess} results for various series of nanocomposites containing POSS nano-cages. Incorporation of untreated POSS–NH_2 (denoted as POSS in Fig. 8) clearly does not affect the C_p^{excess} of the matrix. However, PCL–POSS nanocomposites prepared by *in situ* polymerization or by the masterbatch approach do display an increased C_p^{excess}. Again, these results can be clearly related to the degree of filler dispersion throughout the PCL matrix.

WAXD was employed for the characterization of the dispersion state in POSS-containing PCL nanocomposites. Untreated POSS nano-cages tend to agglomerate and to arrange in a specific crystalline structure characterized by clear WAXD diffraction peaks, as shown in the lower trace of Fig. 9. Individually dispersed POSS nano-cages do not show this specific WAXD pattern and the absence of the characteristic peaks is therefore an indication for a fully dispersed state of individual POSS entities throughout the matrix. Besides the characteristic diffraction peaks of crystalline PCL in the 20–25° 2θ region, the WAXD pattern of PCL filled with 5 wt% of as-received POSS–NH_2 shows some weak diffraction peaks at low diffraction angles, attesting for the occurrence of aggregated POSS structures (see arrows in middle trace of Fig. 9). These characteristic diffraction peaks are no longer observed in PCL filled with 5 wt% of PCL-grafted POSS (MB), evidencing that the filler particles are truly individually dispersed (upper trace in Fig. 9).

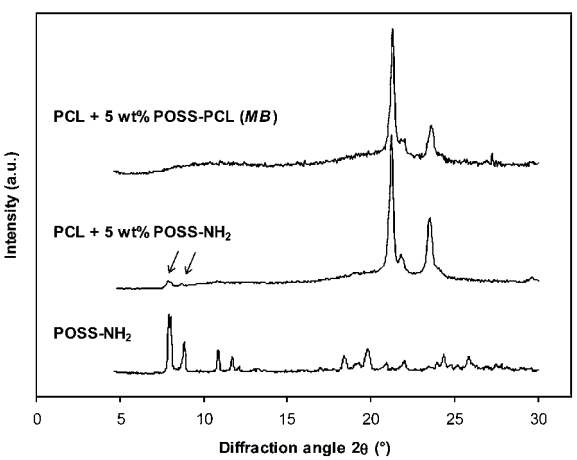

Fig. 9 WAXD profiles of as-received POSS–NH_2 (*lower trace*), and of PCL nanocomposites containing 5 wt% of untreated (*middle trace*) and of PCL-grafted POSS (*upper trace*, grafted chains have a DP = 80). The arrows indicate characteristic diffraction peaks of the aggregated filler.

A closer look at Fig. 8 evidences some additional features. First, let us consider the sample prepared by melt mixing untreated POSS–NH_2 into commercial PCL. Clearly, C_p^{excess} is not at all affected, as expected from the poor dispersion quality (Fig. 9). The situation changes when considering the nanocomposite prepared by *in situ* polymerization (this sample has a POSS content of 9.6 wt% and the grafted PCL chains have a degree of polymerization DP = 80). Compared to the nanocomposites prepared by melt mixing, a marked increase in C_p^{excess} is noticed. This cannot be fully due to the low molar mass of the PCL, since a reference homopolymer sample with a DP of 80 only exhibits a slightly higher C_p^{excess} than the commercial high molar mass PCL (see Fig. 8). Turning to the nanocomposites prepared by the masterbatch approach, we first evaluate the effect of adding low molar mass PCL of DP = 80. The binary mixture of commercial PCL (denoted CAPA) and PCL of DP = 80 shows a slight increase in C_p^{excess} as compared to the commercial PCL alone, reflecting the abovementioned molar mass effect. When POSS–NH_2 is added at 5 wt% loading to prepare a ternary mixture, an additional increase in C_p^{excess} is noticed, suggesting that the presence of low molar mass PCL slightly improves the dispersion state of the untreated POSS. The by far highest increase in C_p^{excess} is noticed, however, when PCL-grafted POSS is incorporated into the commercial PCL matrix (denoted as *melt* POSS–PCL MB DP80 in Fig. 8). It is also worth noting that the use of a POSS–PCL masterbatch with shorter grafted PCL chains, *i.e.*, DP = 40, is less effective in increasing C_p^{excess}. This result indicates that a higher grafted chain length is more efficient in improving the compatibility between POSS nano-cages and the PCL matrix.

Comparison between nanofillers: effect of aspect ratio. When compared to *in situ* nanocomposites based on layered silicates, the C_p^{excess} values attained for *in situ* POSS nanocomposites at equal loading are significantly lower, despite an excellent dispersion state (compare Fig. 6 and 8). It is rather comparable to the value attained for samples in which Cloisite®30B clay was incorporated by melt mixing, but which displayed a lower dispersion quality. Such direct comparison is difficult, however, due to the important difference in the molar masses of the matrix polymer in both cases. Samples prepared by the masterbatch approach therefore provide a more suitable base for comparison, even though minor differences in the PCL molar masses of the different systems subsist.

As a general observation from the comparison between the masterbatch systems in Fig. 6 and 8, it appears that the highest

C_p^{excess} values are observed for layered silicate nanocomposites; POSS and sepiolite systems both have lower C_p^{excess} values. The origin of these differences possibly resides in the aspect ratio of the various considered fillers. We reported previously that the observed C_p^{excess} increases in PCL nanocomposites originate from a modification of the crystalline morphology of the matrix.[27] Because of constraints imposed by the presence of filler particles, PCL spherulites are no longer able to grow freely and the formation of subsidiary rather than primary crystalline lamellae is promoted. The result is a reduced crystal stability, *i.e.*, lower melting temperatures, as well as an alteration to the amount and nature of the crystalline/amorphous interface where reversible melting/crystallization occurs, *i.e.*, increased C_p^{excess}. It was observed that both the *filler type* and its *dispersion state* determine the magnitude of the increase in C_p^{excess}. The dispersion state determines the amount of inorganic '*barriers*' that inhibit the unconstrained lamellar crystal growth, whereas the effect of filler type is related to its aspect ratio, determining the extent of the constraints imposed onto the crystallization of the matrix. Indeed, assuming comparable average inter-particle distances in well-dispersed nanocomposites of all types, *i.e.*, a few tens of nanometres,[46–48] layered silicates with lateral dimensions exceeding 100 nm and an aspect ratio of 70–150 are easily anticipated to have a more profound impact than, for instance, POSS nano-cages with a diameter of only *ca.* 1.3 nm and an aspect ratio of 1. Sepiolite clay, with an aspect ratio of 20–40, is expected to show intermediate behavior. The observed differences between the C_p^{excess} levels attained for the different systems should probably be interpreted in the light of these facts. It is also worth noting, finally, that dispersion state and aspect ratio can even be related to one another, *e.g.*, in systems containing layered silicates, where incomplete exfoliation reduces the effective aspect ratio of the filler particles.

Further evidence for the importance of filler aspect ratio—along with the important effects related to dispersion quality—can be found in the observations on the amorphous fraction of the matrix polymer. In view of the small size and extremely high specific surface of the nano-sized filler particles, the morphological changes resulting from their dispersion are anticipated to be immense. As a result, the altered crystalline morphology, the reduced crystalline perfection and the modified crystalline/amorphous interface also induce the formation of a significant *rigid amorphous fraction* (RAF).[27] Due to its delayed mobility, this amorphous PCL fraction does not devitrify at the glass transition temperature T_g of the bulk, but only upon melting of the constraining crystalline phase at higher temperature. Therefore, when evaluated at the bulk T_g, the magnitude of the heat capacity step associated with the glass transition $\Delta C_p(T_g)$ is reduced for samples containing an important RAF. Fig. 10 shows the $\Delta C_p(T_g)$ determined for unfilled PCL and for several nanocomposites. In order to account for small changes in the degree of crystallinity of the samples, ΔC_p is normalized by dividing it by the percentage of amorphous material (*i.e.*, the amount of non-crystalline material as determined from a DSC heating experiment).

It clearly appears that POSS, incorporated into PCL by either melt mixing or by a masterbatch approach, does not affect the amount of RAF in the PCL matrix. However, sepiolite clay and, even more so, layered silicates do lead to a considerable

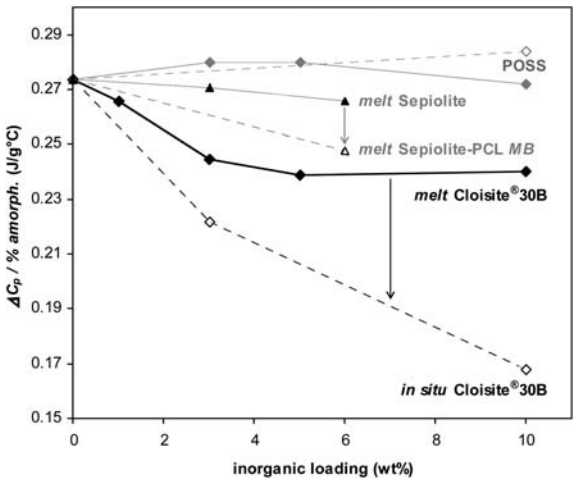

Fig. 10 ΔC_p evaluated at the bulk T_g as a function of filler loading for PCL and various nanocomposites. The arrows illustrate the difference between nanocomposites prepared by melt mixing (*full symbols*) and by the masterbatch (sepiolite, POSS) or *in situ* (layered silicates) approaches (*open symbols*). The values of ΔC_p are normalized for the amount of amorphous polymer in each sample.

reduction in the measured $\Delta C_p(T_g)$ values, to an extent depending on the filler loading and, more importantly, on the degree of filler dispersion (compare nanocomposites by melt mixing and by *in situ* polymerization or masterbatch mixing in Fig. 10). The extent of these changes in the RAF is in good qualitative agreement with the above C_p^{excess} results for the corresponding samples, showing that both phenomena have a common origin, *i.e.*, a semi-crystalline micro-morphology which is substantially affected by the presence of well-dispersed filler particles. These data also further illustrate that improving the degree of filler dispersion, through its connection with the developed polymer microstructure, has a profound impact on the thermal behavior of the material. This appears to be especially pronounced in the presence of high aspect ratio particles. It can therefore be concluded that this parameter strongly contributes to determining the extent of the constraints imposed onto the crystallization of the matrix, thus governing the final achieved crystalline morphology.

Interfacial compatibility: effect of filler modification

So far the discussion focused on how processing conditions and nanocomposite preparation method influence the achievable degree of filler dispersion. However, it is also recognized that—for a given type of nano-sized filler particles—the compatibility between the matrix and the filler plays another key role.[9,10] The present paragraph therefore aims at investigating the influence of various layered silicates, surface-treated by different organic modifiers, on the thermal properties of the PCL matrix. In addition to providing further insight into the effect of *particle aspect ratio* and *interfacial contact surface*, this study also aims at evidencing the importance of *compatibility* issues governing the achievable dispersion state of the filler within the matrix. In order to provide a suitable base for comparison, care was taken to use optimized and reproducible processing conditions for all

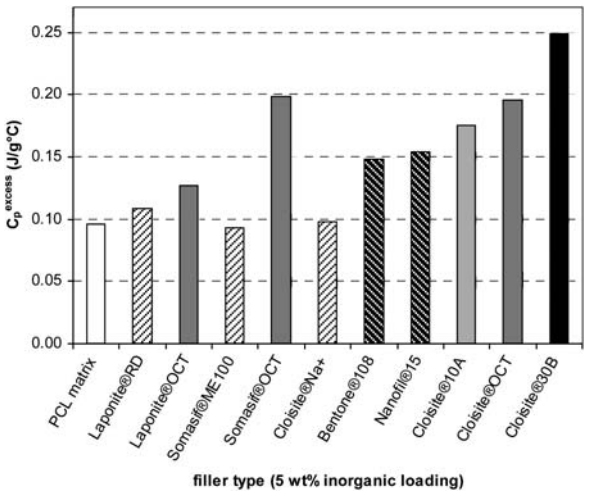

Fig. 11 C_p^{excess} determined from quasi-isothermal crystallization experiments for PCL nanocomposites containing 5 wt% of various types of layered silicates (50 °C, temperature modulation of ±0.5 °C per 60 s).

samples, *i.e.*, high shear rates and sufficiently long residence time in the extruder (30 min).

Fig. 11 shows the excess heat capacity C_p^{excess} determined at the end of a quasi-isothermal crystallization experiment for a series of PCL nanocomposites containing layered silicates. It appears that untreated clays, *i.e.*, Laponite®RD, Somasif®ME100 and Cloisite®Na^+, do not significantly affect C_p^{excess} as compared to the unfilled matrix, which is a consequence of their poor dispersion throughout the PCL matrix. Upon organic modification of the fillers, however, an increase in C_p^{excess} is noticed for all layered silicate types.

The various clays exchanged by dimethyl 2-hydroxyethyl octadecyl ammonium (denoted OCT) allow to visualize the effect of aspect ratio. Laponite®OCT, with a reported aspect ratio of *ca.* 25, only provides a moderate increase in C_p^{excess}, whereas the effect is more pronounced for both Somasif®OCT and Cloisite®OCT, with aspect ratios in excess of 100.[49] The observed tendency agrees well with the above discussion on the importance of aspect ratio.

The effect of surface modification of the filler can be appreciated by comparing differently treated layered silicates. Bentone®108 and Nanofil®15, respectively a natural hectorite and a natural montmorillonite, are both characterized by lateral platelet dimensions in the 70–150 nm range and are exchanged by ammonium cations bearing two aliphatic chains. As observed in Fig. 11, both silicates result in a similar C_p^{excess} increase. The increase is, however, less pronounced than in Cloisite®10A, a natural montmorillonite exchanged with benzyl dimethyl hydrogenated tallowalkyl ammonium. Even though replacing one of the aliphatic chains (as in Nanofil®15 or Bentone®108) by a benzyl group (as in Cloisite®10A) reduces the initial spacing, at the same time it increases the available uncovered clay surface for polar interaction with the PCL matrix. This, in turn, may lead to a better dispersion quality and a more extensively affected matrix/filler interphase, resulting in a higher C_p^{excess} in samples containing Cloisite®10A. An additional increase in C_p^{excess} is observed upon introducing polarity, *e.g.*, by replacing the benzyl group in Cloisite®10A by a more polar hydroxyethyl,

Table 1 WAXD information for PCL samples filled with 5 wt% of various layered silicates, as prepared under optimized melt mixing conditions (30 min residence time at 245 rpm)

Layered silicate	Alkylammonium modifier[a]	d_{001}-spacing	Dispersion state
Cloisite®Na^+	None	1.33 nm	Microcomposite
Cloisite®10A	Benzyl dimethyl hydrogenated tallowalkyl	3.02 nm	Intercalated/ exfoliated
Bentone®108	Dimethyl bis(hydrogenated tallowalkyl)	3.20 nm	Intercalated/ exfoliated
Somasif®OCT	Dimethyl 2-hydroxyethyl octadecyl	3.29 nm	Intercalated/ exfoliated
Cloisite®OCT	Dimethyl 2-hydroxyethyl octadecyl	3.37 nm	Intercalated/ exfoliated
Nanofil®15	Dimethyl dioctadecyl	3.38 nm	Intercalated/ exfoliated
Cloisite®30B	Methyl bis(2-hydroxyethyl) tallowalkyl	n.a.	Fully exfoliated

[a] Hydrogenated tallow: ~65% C_{18}; ~30% C_{16}; ~5% C_{14}.

as in Cloisite®OCT. The highest value of C_p^{excess}, however, is achieved when the organic modifier contains *two* rather than *one* polar hydroxyethyl moieties per ammonium cation, as in Cloisite®30B. The latter is, in addition, the only clay to display a fully disordered, most likely exfoliated morphology under the processing conditions chosen, as appears from the WAXD data listed in Table 1.

The above results clearly evidence the importance of a proper choice of filler modification, dictated by *interfacial compatibility* considerations. On the one hand, the bulkiness of the organic modifier governs the initial spacing of the stacked clay tactoids and may facilitate their delamination (Table 1). On the other hand, the polarity of the modifier determines the affinity between the filler surface and the PCL matrix, which is undoubtedly a prerequisite for effectively increasing the amount of polymer/filler interface, hence, C_p^{excess} (Fig. 11). In this respect, the reported quasi-isothermal crystallization experiments confirm the conclusions from recent reports on poly(amide)-6 and poly(ethylene-*co*-vinyl acetate) nanocomposites.[50,51]

Note, however, that the considerable differences in the measured gallery spacings of the silicates (Table 1) are not reflected in the C_p^{excess} results. This observation clearly shows the limitations of WAXD for evaluating the true dispersion state of the layered silicates, in the sense that it only contains information on the intercalated silicate fraction and does not allow to quantify the amount of individually dispersed platelets. C_p^{excess}, on the other hand, is sensitive to subtle changes in both the dispersion state *and* the aspect ratio of the filler.

Conclusions

An innovative thermal analysis methodology was applied for the characterization of PCL nanocomposites containing layered silicates, needle-like sepiolite, or POSS nano-cages. During quasi-isothermal crystallization experiments, an excess heat

capacity was observed for all samples due to reversible melting and crystallization on the timescale of the imposed MTDSC temperature modulation. It was observed that the magnitude of this C_p^{excess} further increases in the presence of well-dispersed nano-sized filler particles, especially in case they display a high aspect ratio. This effect was attributed to the occurrence of morphological changes induced by the incorporation of the filler particles, promoting the growth of subsidiary PCL crystals and strongly affecting the *amount* and the *nature* of the crystalline/amorphous contact surface within the matrix.

It was furthermore demonstrated that the employed methodology can also be applied for reliably estimating the degree of filler dispersion within the PCL matrix, the modification of the crystalline morphology being a direct consequence of the amount of matrix/filler interface. The method therefore allowed a detailed investigation of the crucial factors affecting the degree of filler dispersion: the choice of processing conditions, the selected nanocomposite preparation method, and the interfacial compatibility between the constituents.

With respect to melt processing conditions, the importance of a sufficiently high residence time within the extruder was evidenced by MTDSC and confirmed by WAXD and DMA data. Moreover, it was shown that increasing the shear stress effectively improves the achieved dispersion state.

The importance of the selected nanocomposite preparation method was demonstrated by comparing nanocomposites prepared by melt mixing, by *in situ* polymerization and by a masterbatch approach. Grafting PCL chains onto the filler was found to strongly enhance its dispersion quality throughout the matrix, not only more strongly affecting C_p^{excess} during quasi-isothermal crystallization, but also significantly increasing the amount of rigid amorphous material, as assessed from non-isothermal MTDSC measurements in the glass transition region of the nanocomposites. As for C_p^{excess}, the amount of material exhibiting a delayed segmental mobility was found to depend upon the aspect ratio of the filler, suggesting that the RAF also finds its origin in the altered crystalline morphology of the PCL matrix.

Finally, interfacial compatibility between the constituents of the nanocomposites was demonstrated to be a most crucial aspect. A comparison between various layered silicates showed that high degrees of filler dispersion in PCL could only be achieved upon polar modification of the silicate, pointing at the importance of a proper choice of the organic silicate modifier.

In conclusion, in addition to highlighting the crucial aspects governing the dispersion state of nano-sized fillers within a polymeric matrix, this work also demonstrated the wide potential of the applied thermal analysis methodology for the characterization of polymeric nanocomposites in general, showing more specifically its high sensitivity towards subtle changes in the amount and nature of the polymer/filler interface.

Acknowledgements

The work of H. E. Miltner was supported by a grant of the Research Foundation Flanders (FWO-Vlaanderen). The authors are grateful to T. Segato and Prof. M.-P. Delplancke (Service de Chimie Industrielle, Université Libre de Bruxelles, Belgium) for WAXD analysis, and to N.-A. Gotzen (Department of Materials and Chemistry, Vrije Universiteit Brussel, Belgium) for AFM imaging. Dr H. Fischer at TNO Industry and Technology (Eindhoven, The Netherlands) is kindly acknowledged for providing access to the extrusion equipment. S. Benali is grateful to 'Région Wallonne' for a grant in the frame of the WINNO-MAT program PROCOMO; UMons acknowledges the financial support from the 'Région Wallonne' and the European Commission (FSE, FEDER) in the frame of Objectif-1 and Phasing-Out programs. This work was partially supported by the Belgian Federal Science Policy Office (PAI6/27) and by the Belgian National Fund for Scientific Research (FRS-FNRS).

Notes and references

1 Y. Kojima, A. Usuki, M. Kawasumi, A. Okada, Y. Fukushima, T. Kurauchi and O. Kamigaito, *J. Mater. Res.*, 1993, **8**, 1185–1189.
2 P. M. Ajayan and T. W. Ebbesen, *Rep. Prog. Phys.*, 1997, **60**, 1025–1062.
3 E. Galan, *Clay Miner.*, 1996, **31**, 443–453.
4 J. D. Lichtenhan, *Comments Inorg. Chem.*, 1995, **17**, 115–130.
5 M. Alexandre and P. Dubois, *Mater. Sci. Eng., R*, 2000, **28**, 1–63.
6 S. S. Ray and M. Okamoto, *Prog. Polym. Sci.*, 2003, **28**, 1539–1641.
7 E. T. L. Thostenson, C. Y. Li and T.-W. Chou, *Compos. Sci. Technol.*, 2005, **65**, 491–516.
8 J. J. Schwab and J. D. Lichtenhan, *Appl. Organomet. Chem.*, 1998, **12**, 707–713.
9 P. Reichert, H. Nitz, S. Klinke, R. Brandsch, R. Thomann and R. Mülhaupt, *Macromol. Mater. Eng.*, 2000, **275**, 8–17.
10 T. D. Fornes, P. J. Yoon, D. L. Hunter, H. Keskkula and D. R. Paul, *Polymer*, 2002, **43**, 5915–5933.
11 C. Velasco-Santos, A. L. Martinez-Hernandez and V. M. Castano, *Compos. Interfaces*, 2005, **11**, 567–586.
12 D. Tasis, N. Tagmatarchis, A. Bianco and M. Prato, *Chem. Rev.*, 2006, **106**, 1105–1136.
13 J. W. Cho and D. R. Paul, *Polymer*, 2001, **42**, 1083–1094.
14 G. S. Rajan, G. S. Sur, J. E. Mark, D. W. Schaefer and G. Beaucage, *J. Polym. Sci., Part B: Polym. Phys.*, 2003, **41**, 1897–1901.
15 X. H. Liu and Q. J. Wu, *Polymer*, 2001, **42**, 10013–10019.
16 S. H. Qin, D. Q. Qin, W. T. Ford, D. E. Resasco and J. E. Herrera, *Macromolecules*, 2004, **37**, 752–757.
17 A. Usuki, Y. Kojima, M. Kawasumi, A. Okada, Y. Fukushima, T. Kurauchi and O. Kamigaito, *J. Mater. Res.*, 1993, **8**, 1179–1184.
18 P. B. Messersmith and E. P. Giannelis, *J. Polym. Sci., Part A: Polym. Chem.*, 1995, **33**, 1047–1057.
19 R. K. Shah and D. R. Paul, *Polymer*, 2004, **45**, 2991–3000.
20 B. Lepoittevin, N. Pantoustier, M. Devalckenaere, M. Alexandre, C. Calberg, R. Jérôme, C. Henrist, A. Rulmont and P. Dubois, *Polymer*, 2003, **44**, 2033–2040.
21 P. Brocorens, S. Benali, C. Broekaert, F. Monteverde, H. E. Miltner, B. Van Mele, M. Alexandre, P. Dubois and R. Lazzaroni, *Langmuir*, 2008, **24**, 2072–2080.
22 S. Benali, S. Peeterbroeck, P. Brocorens, F. Monteverde, L. Bonnaud, M. Alexandre, R. Lazzaroni and P. Dubois, *Eur. Polym. J.*, 2008, **44**, 1673–1685.
23 W. Lertwimolnun and B. Vergnes, *Polym. Eng. Sci.*, 2007, **47**, 2100–2109.
24 F. Chavarria, R. K. Shah, D. L. Hunter and D. R. Paul, *Polym. Eng. Sci.*, 2007, **47**, 1847–1864.
25 N. Grossiord, O. Regev, J. Loos, J. Meuldijk and C. E. Koning, *Anal. Chem.*, 2005, **77**, 5135–5139.
26 B. Lepoittevin, M. Devalckenaere, N. Pantoustier, M. Alexandre, D. Kubies, C. Calberg, R. Jérôme and P. Dubois, *Polymer*, 2002, **43**, 4017–4023.
27 H. E. Miltner, N. Watzeels, A.-L. Goffin, E. Duquesne, S. Benali, B. Ruelle, S. Peeterbroeck, P. Dubois and B. Van Mele, *Macromolecules*, 2010, submitted.
28 A.-L. Goffin, E. Duquesne, J.-M. Raquez, H. E. Miltner, X. Ke, M. Alexandre, G. Van Tendeloo, B. Van Mele and P. Dubois, *J. Mater. Chem.*, 2010, DOI: 10.1039/c0jm00283f.
29 E. Duquesne, S. Moins, M. Alexandre and P. Dubois, *Macromol. Chem. Phys.*, 2007, **208**, 2542–2550.

30 H. E. Miltner, N. Watzeels, C. Block, N.-A. Gotzen, G. Van Assche, K. Borghs, K. Van Durme, B. Van Mele, B. Bogdanov and H. Rahier, *Eur. Polym. J.*, 2010, **46**, 984–996.
31 P. Liu and J. Guo, *Colloids Surf., A*, 2006, **498**, 282–283.
32 B. Lepoittevin, N. Pantoustier, M. Devalckenaere, M. Alexandre, D. Kubies, C. Calberg, R. Jérôme and P. Dubois, *Macromolecules*, 2002, **35**, 8385–8390.
33 A.-L. Goffin, E. Duquesne, S. Moins, M. Alexandre and P. Dubois, *Eur. Polym. J.*, 2007, **43**, 4103–4113.
34 B. Lepoittevin, N. Pantoustier, M. Alexandre, C. Calberg, R. Jérôme and P. Dubois, *J. Mater. Chem.*, 2002, **12**, 3528–3532.
35 H. E. Miltner, H. Rahier, A. Pozsgay, B. Pukánszky and B. Van Mele, *Compos. Interfaces*, 2005, **12**, 787–803.
36 H. E. Miltner, G. Van Assche, A. Pozsgay, B. Pukánszky and B. Van Mele, *Polymer*, 2006, **47**, 826–835.
37 H. E. Miltner, S. Peeterbroeck, P. Viville, P. Dubois and B. Van Mele, *J. Polym. Sci., Part B: Polym. Phys.*, 2007, **45**, 1291–1302.
38 K. Ishikiriyama and B. Wunderlich, *J. Polym. Sci., Part B: Polym. Phys.*, 1997, **35**, 1877–1886.
39 A. A. Minakov and C. Schick, *Thermochim. Acta*, 1999, **330**, 109–119.
40 R. Scherrenberg, V. Mathot and A. Van Hemelrijck, *Thermochim. Acta*, 1999, **330**, 3–19.
41 M. Reading, A. Luget and R. Wilson, *Thermochim. Acta*, 1994, **238**, 295–307.
42 B. Wunderlich, Y. Jin and A. Boller, *Thermochim. Acta*, 1994, **238**, 277–293.
43 A. Wurm, M. Merzlyakov and C. Schick, *J. Therm. Anal. Calorim.*, 1999, **56**, 1155–1161.
44 *The Advanced Thermal Analysis System (ATHAS) Databank*, ed. M. Pyda, http://athas.prz.edu.pl/.
45 G. Ozkoc, G. Bayram and M. Quaedflieg, *J. Appl. Polym. Sci.*, 2008, **107**, 3058–3070.
46 M. A. van Es, Polymer-Clay Nanocomposites. The Importance of Particle Dimensions, PhD thesis, Technische Universiteit Delft, 2001.
47 R. Krishnamoorti and R. A. Vaia, *J. Polym. Sci., Part B: Polym. Phys.*, 2007, **45**, 3252–3256.
48 J. N. Coleman, U. Khan and Y. K. Gun'ko, *Adv. Mater.*, 2006, **18**, 689–706.
49 Y. J. Xu, W. J. Brittain, C. C. Xue and R. K. Eby, *Polymer*, 2004, **45**, 3735–3746.
50 T. D. Fornes, D. L. Hunter and D. R. Paul, *Macromolecules*, 2004, **37**, 1793–1798.
51 L. Cui, X. Y. Ma and D. R. Paul, *Polymer*, 2007, **48**, 6325–6339.

